Report no. 07/21

Linear Instability of asymmetric Poiseuille flows

Dick Kachuma & Ian J. Sobey

We compute solutions for the Orr-Sommerfeld equations for the case of an asymmetric Poiseuille-like parallel flow. The calculations show that very small asymmetry has little effect on the prediction for linear instability of Poiseuille-like flow but that moderate asymmetry, such as found in channel flow near an elongated wall vortex, has a large effect and that instability can occur at much lower (less than 100) Reynolds numbers. We give some characterisation of the instability.

Oxford University Computing Laboratory
Numerical Analysis Group
Wolfson Building
Parks Road
Oxford, England OX1 3QD

November, 2007

1 Introduction

Computation of fast moving waves in a laminar channel flow (Kachuma (2007)) have shown the growth of what appears to be a Kelvin-Helmholtz instability in the flow. In this paper we examine solutions of the Orr-Sommerfeld equation for a parallel flow that is a model for the more complicated channel flow. We show that linear instablities should occur at relatively low Reynolds number and examine the characteristics of the developing disturbances.

Linear stability theory played a key role in the development of fluid mechanics during much of the twentieth century. However, towards the end of the century it became apparent that core information about the evolution of fluid flows needed more complicated ideas. There were a number of important reasons for this. One was the ability to compute solutions of the laminar Navier–Stokes equations, making linearised models, usually in highly idealised geometries, seem irrelevant to complex flows in complex geometries. Another reason was that growing realisation of the importance of non-linear effects and the development and understanding of bifurcation theory meant that the limitations of what could be described by linearised models were better appreciated (Stewartson & Stuart (1971); Stuart (1971)). A further, and perhaps theoretically most important factor was the realisation that the predictions of linearised theory when applied to channel and pipe flows seemed to be not in accord with observed flows (Davies & White (1928); Patel & Head (1969); Carlson *et al.* (1982); Lundbladh & Johansson (1991); Tillmark & Alfredsson (1992); Klebanoff *et al.* (1962); Orszag & Patera (1983); Bayly *et al.* (1988)). Recent ideas (Trefethen *et al.* (1993)) predict that non-normality of the Navier–Stokes operator can lead to enormous transient amplification of disturbances regardless of whether the flow is stable or unstable to linearised disturbances. In this paper we show that the symmetric Poiseuille flow is in a sense a special situation and that if the flow has a moderate asymmetric disturbance then solutions of the Orr-Sommerfeld equation predict instablity and growth rates that may be in accord with transient growth calculations from the full Navier–Stokes equations at quite low Reynolds numbers.

Linear stability theory has been applied to a number of parallel flows, particularly Couette and Poiseuille flow that are physically realisable flows. The theory has also been applied to model nearly parallel flows such as a shear layer where there is a smooth transition between two uniform velocities. Such flow is not physically realisable (since the pressure should vary across the flow in a way that cannot be achieved in a parallel flow) but is a reasonable model for nearly parallel flow where the length scale for changes in the flow direction is much larger than the width of the shear layer. In this paper we show that in a channel flow, there is a region near a wall vortex, particularly the second vortex, where the flow is almost parallel over a length that is sufficiently large compared to the channel width for a parallel flow model to be applied.

In computing solutions to two-dimensional flow through a channel with an asymmetric step expansion, it is well known that in addition to the primary vortex behind the step, as the Reynolds number increases, a secondary vortex forms on the opposite wall, see for example Sobey (1985); Tutty & Pedley (1993). In Figure 1 we show an example flow from a finite difference solution of the Navier–Stokes equations at a

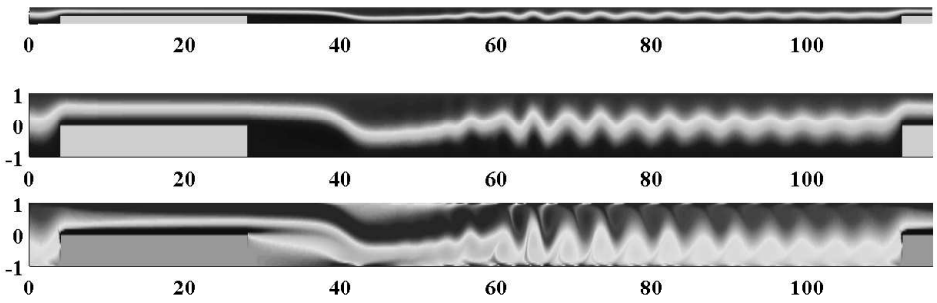

Figure 1: Example computed two-dimensional flow past a step showing in the upper two diagrams greyscale contours for the streamfunction and in the lowest diagram contours of the vorticity and in particular an unstable flow developing from the vorticity layers around the secondary vortex. The flow is from a computed solution of Navier–Stokes equations at a Reynolds number of 400 with 50880 uniformly distributed mesh points in a longitudinally periodic configuration. The region of interest in this paper is for longitudinal values in the range 40 to 60.

Reynolds number 400 (based on average velocity and half minimum channel width) in a periodic geometry where an instablity emerges from the secondary vortex. The figure shows shaded contour plots for the stream-function (upper two diagrams, note that the vertical axis of the lower figures are stretched for clarity) and the vorticity. Our interest here is in regions where the base flow is essentially parallel but with a reverse velocity on one wall. In the figure there is a very apparent instability which develops in the flow around the secondary vortex, leading to a train of vortices further downstream. The lower diagram shows a deformation of two vorticity layers that is extremely suggestive of a Kelvin-Helmholz instability mechanism.

In the next scetion we formulate a standard Orr-Sommerfeld equation for the model situation, giving a little more detail to justify a local paralllel flow approximation. We then present the main results and give a few summary comments.

2 Formulation

We start by considering the governing equations for small disturbances in parallel flow. We define a base velocity field $\mathbf{U} = (U(y), 0)^T$ as a parallel flow in a plane channel. The channel walls are considered flat located at $y = \pm 1$ in non-dimensional units.

If the underlying flow is steady or very slowly varying then then normal mode analysis can be done by considering disturbance to the stream function of the form

$$\psi(x, y, t) = \phi(y) \mathrm{e}^{\mathrm{i}(kx - \omega t)}, \tag{2.1}$$

which results in the classical Orr-Sommerfeld equation (Drazin (2002))

$$(U - c)\left(\phi'' - k^2\phi\right) - U''\phi = \frac{1}{\mathrm{i}k\mathrm{R}e}\left(\phi^{(4)} - 2k^2\phi'' + k^4\phi\right), \tag{2.2}$$

where $c = \omega/k$ is the speed of propagation and ϕ has the boundary conditions

$$\phi(\pm 1) = \phi'(\pm 1) = 0. \tag{2.3}$$

The flow U is unstable if disturbances at a particular wave number grow in amplitude with time. That is to say if the imaginary part of c, c_i is positive for a positive wave number k. The eigenvalues c are dependent on the underlying flow $U(y)$, the wave number k and the Reynolds number Re.

The Orr-Sommerfeld equation for plane Poiseuille flow has been extensively studied (for example Orszag (1971)). He reports a critical Reynolds number of R$e_c = 5772$ and critical wave number $k_c = 1.0255$ for plane Poiseuille flow, $U(y) = 1 - y^2$. Such symmetric flows are very stable and in the unstable regimes, have very slow growth rates. For example Poiseuille flow $U(y) = 1 - y^2$ at R$e = 10^4$ has a maximum growth parameter $c_i = 1.310 \times 10^{-2}$ which would require almost 10 cycles to grow by an order of magnitude.

However, we consider the effect of asymmetry of the underlying flow. The underlying flow is modelled as

$$U(y) = \frac{15}{2}\frac{1}{5 - \sigma_2}(1 - y^2)(1 - \sigma_1 y - \sigma_2 y^2), \tag{2.4}$$

where σ_1 and σ_2 are model parameters. For $\sigma_1 = \sigma_2 = 0$ the flow is plane Poiseuille and the multiplicative factor is to ensure that the flux is maintained at

$$\int_{-1}^{1} U(y)\,\mathrm{d}y = 2. \tag{2.5}$$

Thus the base flow U is still considered parallel but is no longer symmetric as Poiseuille flow. By varying the model parameters σ_1 and σ_2, the characteristics of the base flow and consequently its stability should vary. The effect of the parameter σ_1 is simply to change the skewness of the profile. The second order parameter σ_2 on the other hand affects the maximum value of $U(y)$. It should also be pointed out that for certain choices of σ_1 and σ_2 the flow develops backward flow near the channel walls. In particular for $\sigma_1 = 1.5$ and $\sigma_2 = 0$ the flow has a minimum velocity $U(y) = -0.11482$ at $y = 0.84088$. Typical profiles are illustrated in Figure 2 for a range of values for σ_1 and σ_2.

That such a velocity profile might be reasonable comes from observations of computed flows in asymmetric channels. As shown in Figure 3 (a) the steady flow through a channel with a sudden asymmetric step exhibits regions in which the flow is not symmetric but nonetheless nearly parallel. To determine how well the model flow approximates the numerically computed flow, a least squares fit is performed to determine σ_1 and σ_2 that correspond to the computed Navier–Stokes solution. Thus given a flow field $(u(x, y), v(x, y))^T$ computed from solving the Navier–Stokes equations values $\sigma_1(x)$ and $\sigma_2(x)$ are computed for each streamwise point x such that

$$e(x) = \int_{-1}^{1} |u(x, y) - U(y)|^2\,\mathrm{d}y, \tag{2.6}$$

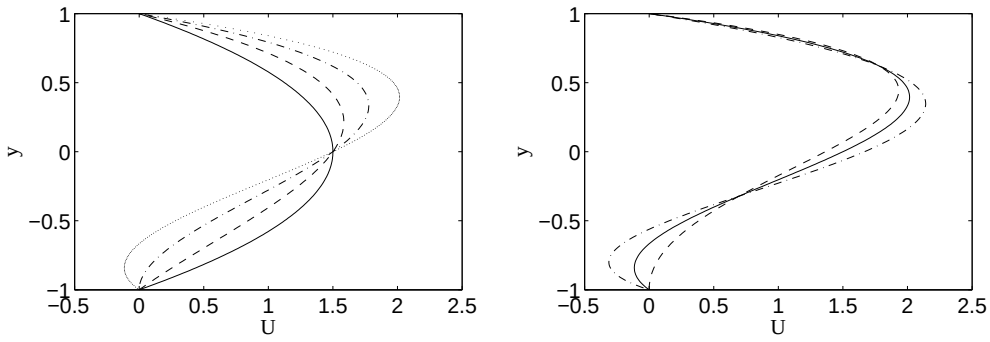

(a) (b)

Figure 2: Example underlying velocity profiles: (a) Fixed $\sigma_2 = 0$: (—) $\sigma_1 = 0$ [Poiseuille flow], (- - -) $\sigma_1 = -0.5$, (- · -) $\sigma_1 = -1.0$, ($\cdots$) $\sigma_1 = -1.5$, (b) Fixed $\sigma_1 = -1.5$: (—) $\sigma_2 = 0$. (- - -) $\sigma_2 = 0.5$, (- · -) $\sigma_2 = -0.5$.

is minimised, where U is defined by (2.4). The minimum value of $e(x)$ measures how good the model fits the flow field. To assess how accurately the parallel flow assumption is satisfied we use the function $d(x)$ defined by

$$d(x) = \frac{||v(x,\cdot)||}{||u(x,\cdot)||}, \tag{2.7}$$

where the norm is the discrete maximum norm. Smaller values of $d(x)$ indicate that at that streamwise location, vertical velocities are negligible as compared to streamwise velocities and hence, locally, the flow is nearly parallel.

The model is compared to a numerically computed flow in Figure 3.

Figure 3 (a) shows a contour plot of the stream function ψ for a steady flow with R$e = 200$. The streamlines indicate regions in the flow field near $x = 13$ shaded in gray where the flow is nearly parallel. It should be noted that the vertical scale is exaggerated and thus the regions of nearly parallel flow are quite long.

Figure 3 (b) shows a slow variation of both σ_1 and σ_2 with x and that both approach zero further downstream showing the development of Poiseuille flow downstream. For small values of x, typically $x < 5$, σ_1 and σ_2 are large. In this region, near the channel expansion, the flow does not match the model, as can be seen from the large values of $e(x)$ in Figure 3 (c). Further downstream, $e(x)$ is decreasing indicating an improved fit in the model. In this region the values of σ_1 and σ_2 vary smoothly in the interval $[-2, 2]$, and further study is limited to this interval.

Figure 3 (d) shows the degree of parallelism in the flow measured by $d(x)$ as defined in (2.7). This shows small values indicating strong parallelism especially further downstream of the expansion where the flow switches to Poiseuille flow. There is also a sharp decrease in $d(x)$ in the vicinity of the centre of the secondary vortex (the shaded region) and it is here that the model is most applicable.

We have solved the steady Orr-Sommerfeld eigenvalue problem (2.2)-(2.3) using the spectral collocation method of Schmid & Henningson (2001). This involves discretis-

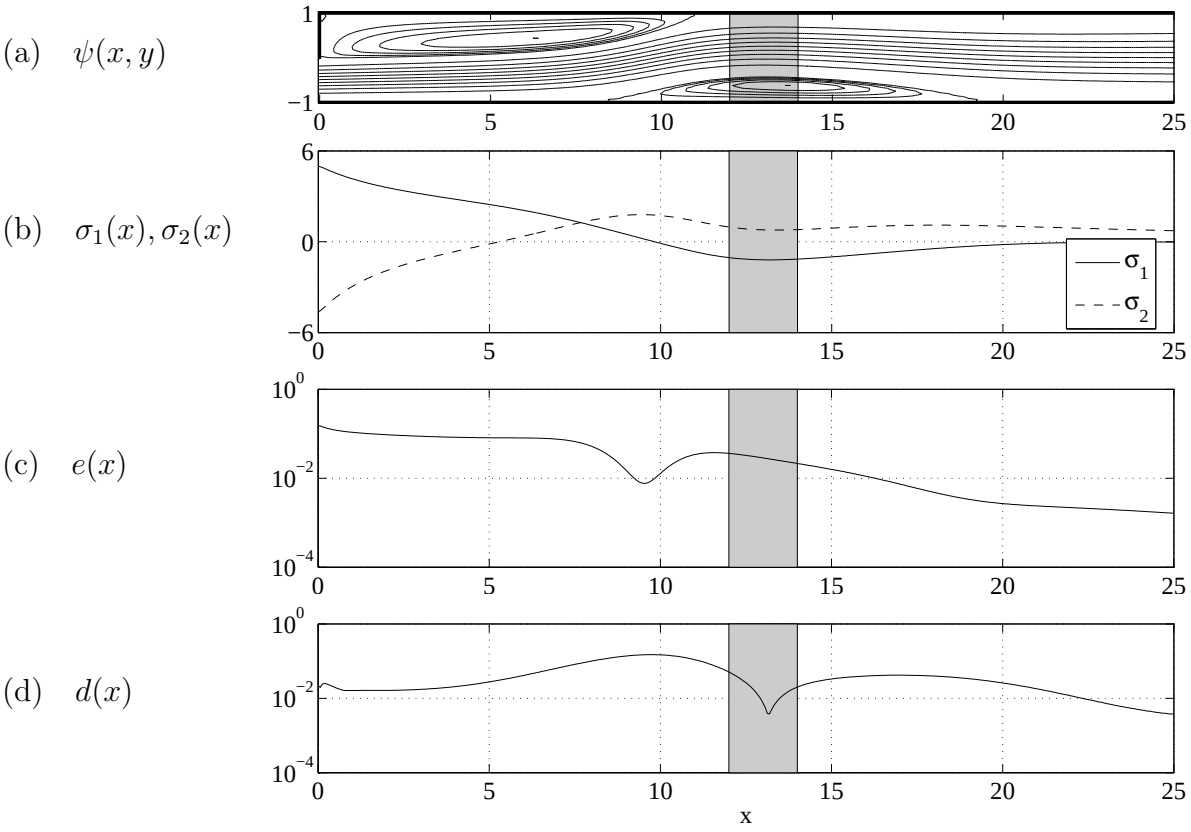

Figure 3: Solution for Navier–Stokes equation at $Re = 200$ and least squares fit of parameters for (2.4). (a) streamlines of numerically computed solution for steady flow, (b) variation of parameters σ_1 and σ_2 along the channel, (c) measure of goodness of fit of model equation (2.4) to actual longitudinal velocity, (d) measure of non-paralleism in flow. The shaded region shows areas near the secondary vortex where the flow is nearly parallel.

ing the spatial operators using Chebyshev polynomials and casting the problem as a generalised matrix eigenvalue problem. This has then been solved using MATLAB's generalised eigenvalue solver which uses generalised Schur decomposition to compute the eigenvalues (Anderson *et al.* (1999)). Pseudospectra are computed using `eigtool` (see Wright & L.N.Trefethen (2002)).

3 Stability results

Figure 4 shows the stability diagrams for the model flow (2.4) for different values of σ_1 and σ_2. The diagram has the Reynolds number on the horizontal axis and the the wave number on the vertical axis. The shaded region in each figure is the unstable region and this is separated from the stable region by the dotted neutral stability curve. In the unstable region, modes at the particular wave number grow in time for a flow at the prescribed Reynolds number.

The general trend in Figure 4 is that both σ_1 and σ_2 alter the stability characteristics of the model flow. The way in which this change is performed is however different. Since σ_1 simply changes the symmetry of the flow, positive and negative values of σ_1 have the same effect on stability so it suffices to consider only positive values of σ_1. Large values of σ_1 can be seen to be destabilising with the unstable region growing in extent as σ_1 increases. For σ_2 however the situation is different. Whereas positive values are destabilising, negative values generally stabilise the flow.

The solid curves in Figure 4 indicate the dominant wave number for each Reynolds number. In certain cases especially for $\sigma_1 = 0.5$ and $\sigma_2 = -0.1$ there is a sudden shift in the dominant wave number indicated by a unsmooth solid curve. This indicates a switch between two Airy modes as labelled by Mack (1976).

The critical Reynolds number also depends on the model parameters σ_1 and σ_2. For steady Poiseuille flow $U(y) = 1 - y^2$, Orszag (1971) computed the historical critical Reynolds number $\mathrm{R}e_c = 5772.22$ which corresponds to $\mathrm{R}e_c = 3848.15$ for our scaling $U(y) = \frac{3}{2}(1 - y^2)$. Such values for the critical Reynolds number give the impression that the plane channel flows at Reynolds numbers less than 10^3 should be linearly stable with all wave components being damped. Furthermore the growth rates predicted by Poiseuille flow analysis in the unstable region are very small so that growth of instabilities is unobservable at short time scales.

However, due to lack of symmetry evidenced by nonzero values of σ_1 and σ_2, the Reynolds numbers at which the flow becomes linearly unstable are reduced. This is shown in Figure 5 which shows the critical Reynolds number $\mathrm{R}e_c$ and the critical wave number k_c for the model flow (2.4) with different values of σ_1 and σ_2. As noted before negative values of σ_2 are stabilising, increasing $\mathrm{R}e_c$ while positive values reduce $\mathrm{R}e_c$. The general trend in the diagrams is that the critical Reynolds number initially increases with σ_1 but there is a critical value of σ_1 around $\sigma_1 \approx 0.5$ when there is a sharp decrease in the critical Reynolds number with σ_1. This decreasing trend in $\mathrm{R}e_c$ continues with increasing σ_1 so that for large values of σ_1, the critical Reynolds number is well under $\mathrm{R}e_c = 100$.

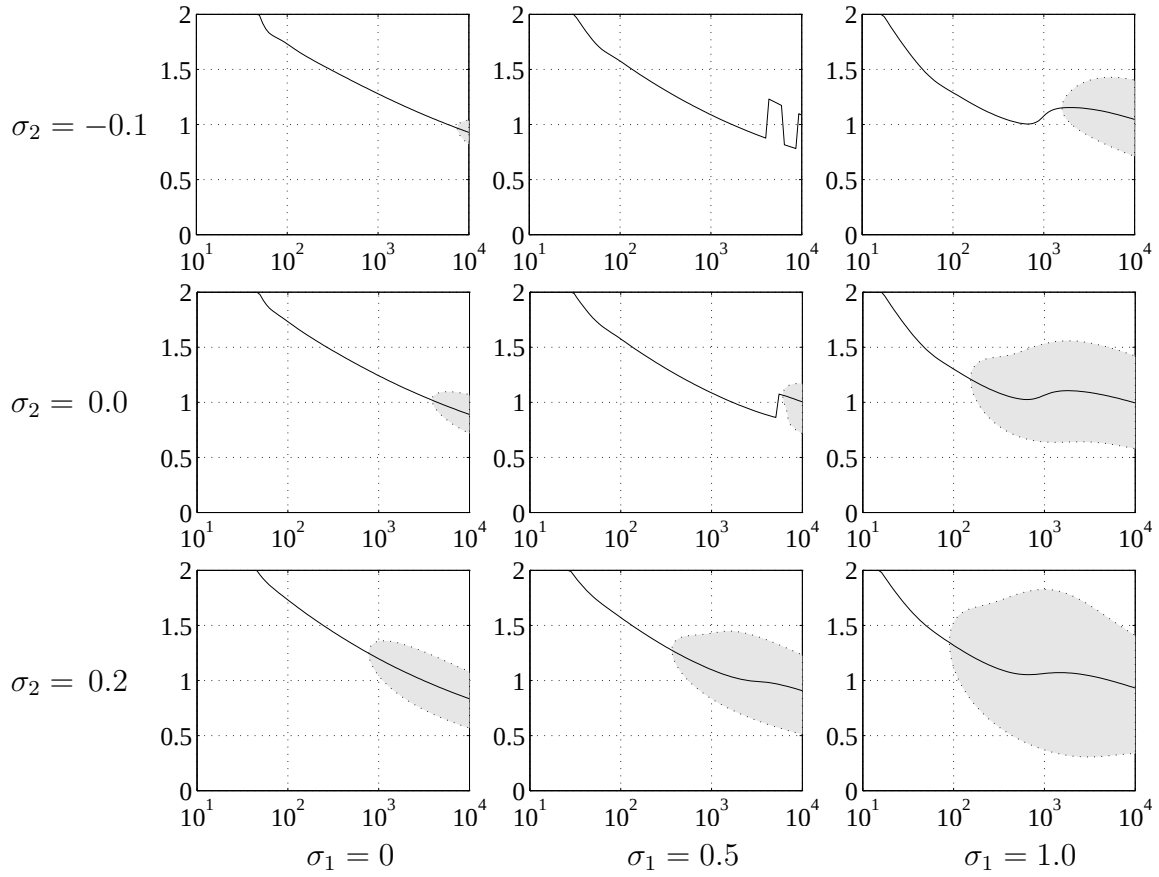

Figure 4: Stability curves for model flow (2.4) for different values of model parameters σ_1 and σ_2. The diagrams have Reynolds number Re on the horizontal axis and wave number k on the vertical axis. The gray area indicates the linearly unstable region while the white region is the stable region. The solid curve in each diagram indicates the most dominant wave number at each Reynolds number. Note that the location of the least stable eigenvalue appears to jump between values when $\sigma_1 = 0.5$. The critical Reynolds number for instability is graphed in Figure 5.

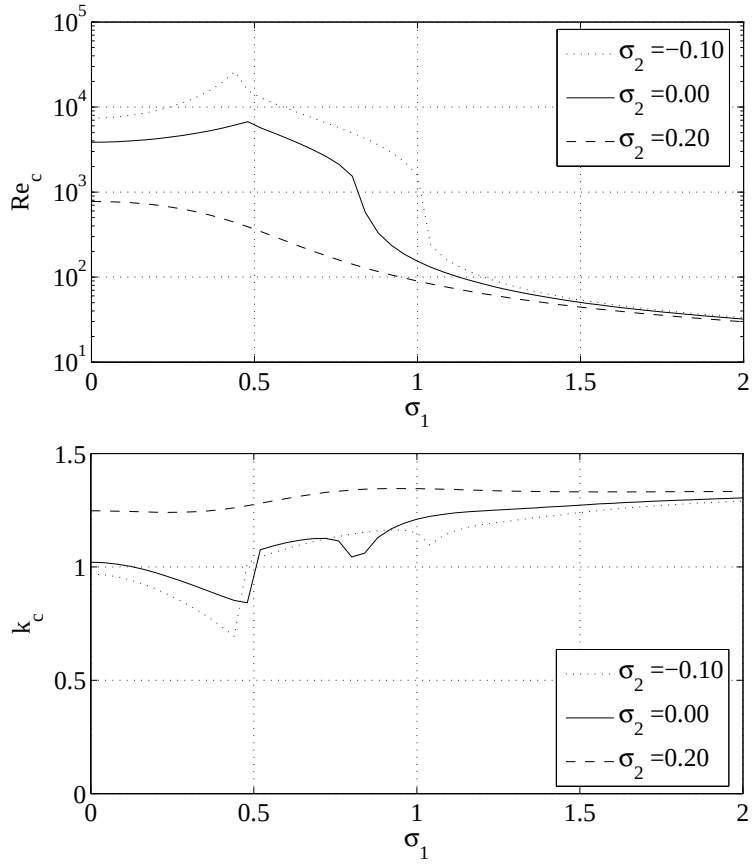

Figure 5: Variation of the critical Reynolds number $\mathrm{R}e_c$ and wave number k_c with the asymmetry parameter σ_1 for three values of the second parameter σ_2.

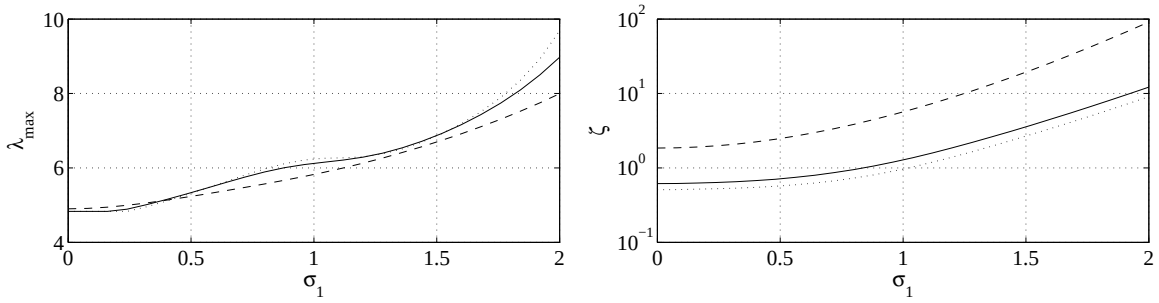

Figure 6: Characteristics of the dominant mode for flow with Re = 600. The lowest diagram shows the growth per cycle of the instability which when $\sigma_1 = 1.5$ is an order of magnitude larger than for plane Poiseuille flow. $\sigma_2 = -0.1$ $(\cdots)$, $\sigma_2 = 0$ $(---)$, $\sigma_2 = 0.2$ $(---)$.

For predictions of the growth rates, we observe that the disturbance is essentially like

$$\psi_1 \sim \mathrm{e}^{kc_i t}\mathrm{e}^{\mathrm{i}k(x-c_r t)} \tag{3.1}$$

so that the wavelength of a disturbance is $\lambda = 2\pi/k$, the temporal frequency of a disturbance is $\omega = kc_r$ and the amplification per cycle, which we denote by ζ, is

$$\zeta = \mathrm{e}^{2\pi c_i/c_r}. \tag{3.2}$$

These values are shown in Figure 6 which has the curves of the wavelength λ, the temporal frequency ω and the growth rate per cycle ζ of the most dominant mode for a flow with Re = 600 for different values of σ_1 and σ_2.

The growth per cycle ζ is large for $\sigma_1 > 1$ even for $\sigma_2 = 0$. The maximum rate for $\sigma_1 = 1$ is $\zeta = 1.2864$ and for $\sigma_1 = 1.5$ is $\zeta = 3.4215$. This indicates that the disturbances grow in amplitude by an order of magnitude in just three cycles. For larger values of σ_1, say $\sigma_1 = 2$ such a growth can be achieved in just one cycle. If the parameter σ_2 is increased, the growth rates are even more excessive with the flow becoming unstable for all values of σ_1 at $\sigma_2 = 0.5$. For $\sigma_1 = 2$ and $\sigma_2 = 0.5$ the disturbance will grow by two orders of magnitude in just one cycle.

This should be compared to Poiseuille flow $U = \frac{3}{2}(1 - y^2)$ at Re = 6666.67 (which corresponds to Re = 10^4 for $U = 1 - y^2$) has a maximum growth rate $\zeta = 1.1266$. Even at such large Reynolds numbers such a disturbance would require at least eight cycles to grow by an order of magnitude. Furthermore at the low Reynolds numbers considered in this work the flows are linearly stable.

4 Eigenvalues and Pseudospectra

We have computed the eigenvalue spectra and pseudospectrum for the Orr-Sommerfeld operator with the asymmetric velocity profile. The eigenvalue spectra are very similar to those computed by Reddy *et al.* (1993); Dongarra *et al.* (1996) for Poiseuille flow and indeed while Reddy *et al.* (1993) considered the effect of small disturbances on the structure

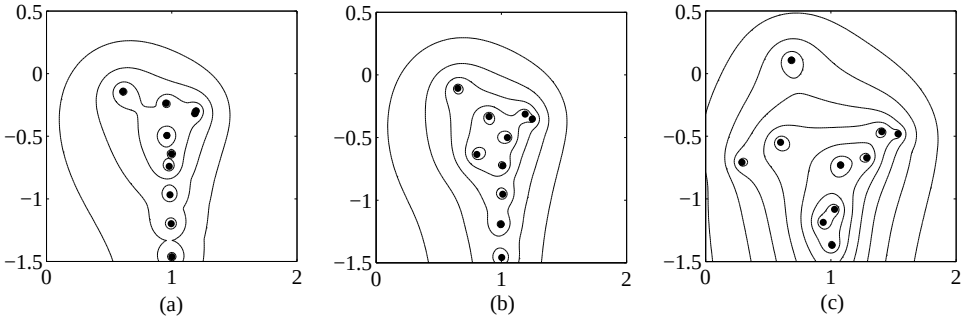

Figure 7: Eigenvalues and pseudospectra for $Re = 200$, $k = 1$, $\sigma_2 = 0$: (a) $\sigma_1 = 0$ (Poiseuille flow), (b) $\sigma_1 = -0.5$, (c) $\sigma_1 = -1.5$

of the pattern of eigenvalues, here even with much larger deviations from the symmetric flow situation, the pattern of eigenvalues retains much of the original structure.

In Figure 7 we show the location of eigenvalues in the complex plane when $Re = 200$ and for the asymmetry parameter varying between $\sigma_1 = 0$ [Poiseuille flow] and $\sigma_1 = -1.5$, as well as pseudospectra (the outer contour is for $\epsilon = 10^{-1}$ and then towards the eigenvalues, $\epsilon = 10^{-1.5}, 10^{-2}, \ldots$. The main feature of these plots is that a single eigenvalue crosses the line $Im(c) = 0$ leading to instability with a single well defined eigenmode. Before instablity occurs (as σ_1 varies) the pseudospectra show only a little non-normality (as ϵ is relatively large, order 0.1) so the transition from stable to unstalbe should be well indicated by the sign on the imaginary part of the eigenvalue changing sign. In figure 8, plots are drawn for the same variation of σ_1 but for amuch larger Reynolds number, $Re = 1000$. Here there is a similar picture for variation of the eigenvalues, a single eignevalue crosses the line $Im(c) = 0$ as σ_1 changes. The pseudospectra contours show that non-normality is becoming more important although still relatively weak at this Reynolds number.

5 Conclusion

We have examined a parallel flow model for flow in an elongated vortex in a channel flow using the Orr-Sommerfeld formulation. The results show that while small asymmetry has, if anything, a stabilising effect, larger asymmetry results in linear instablity at a much reduced Reynolds number. Even more important for practical purposes, as the asymmetry increases, the growth rate of disturbances becomes large enough for this instablity mechanism to be seen as the source of the train of eddies that can develop in channel flow. This analysis shows that linear stability analysis may be a basis for understanding development of these disturbances in two-dimensional channel flows.

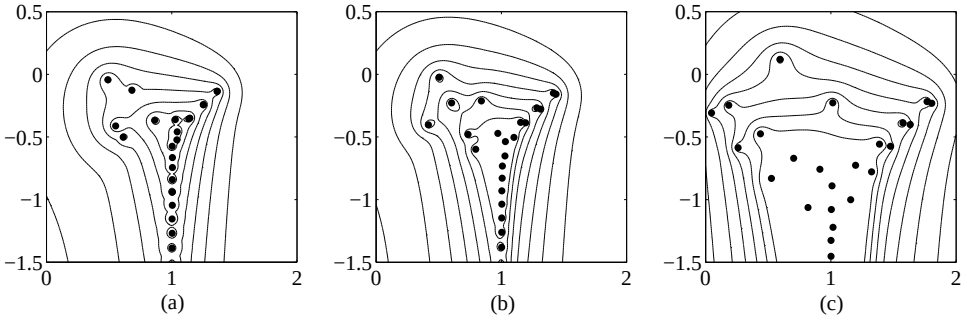

Figure 8: Eigenvalues and pseudospectra for $Re = 1000$, $k = 1$, $\sigma_2 = 0$: (a) $\sigma_1 = 0$ (Poiseuille flow), (b) $\sigma_1 = -0.5$, (c) $\sigma_1 = -1.5$

References

Anderson, E., Bai, Z., Bischof, C., Blackford, S., Demmel, J., Dongarra, J., Croz, J. Du, Greenbaum, A., Hammarling, S., McKenney, A. & Sorensen, D. 1999 *LAPACK User's Guide*. SIAM.

Bayly, B. J., Orszag, S. A. & Herbert, T. 1988 Instability mechanisms in shear-flow transition. *Annual Review of Fluid Mechanics* **20**, 359–391.

Carlson, D. R., Widnall, S. E. & Peeters, M. F. 1982 A flow-visualization study of transition in plane poiseuille flow. *Journal of Fluid Mechanics* **121**, 487–505.

Davies, S. J. & White, C. M. 1928 An experimental study of the flow of water in pipes of rectangular section. *Royal Society of London Proceedings Series A* **119**, 92–107.

Dongarra, J.J., Straughan, B. & Walker, D.W. 1996 Chebyshev tau-qz algorithm methods for calculating spectra of hydrodynamic stability problems. *Applied Numerical Mathematics* **22**, 399–434.

Drazin, P. G. 2002 *Introduction to Hydrodynamic Stability*. Cambridge University Press.

Kachuma, Dick 2007 Fast moving waves in two-dimensional channel flow. PhD thesis, University of Oxford.

Klebanoff, P. S., Tidstrom, K. D. & Sargent, L. M. 1962 The three-dimensional nature of boundary layer instability. *Journal of Fluid Mechanics* **12**, 1–34.

Lundbladh, A. & Johansson, A. V. 1991 Direct simulation of turbulent spots in plane couette flow. *Journal of Fluid Mechanics* **229**, 499–516.

Mack, Leslie M. 1976 A numerical study of the temporal eigenvalue spectrum of the blasius boundary layer. *Journal of Fluid Mechanics* **73**, 497–520.

Orszag, Stephen A 1971 Accurate solution of the orr-sommerfeld stability equation. *Journal of Fluid Mechanics* **60**, 689–703.

Orszag, S. A. & Patera, A. T. 1983 Secondary instability of wall-bounded shear flows. *Journal of Fluid Mechanics* **128**, 347–385.

Patel, V. C. & Head, M. R. 1969 Some observations on skin friction and velocity profiles in fully developed pipe and channel flows. *Journal of Fluid Mechanics* **38**, 181–201.

Reddy, S.C., Schmid, P.J. & Henningson, D.S. 1993 Psuedospectra of the orr–somerfeld operator. *SIAM Journal on Applied Mathematics* pp. 15–47.

Schmid, Peter J & Henningson, Dan S 2001 *Stability and Transition in Shear Flows*. Springer-Verlag.

Sobey, Ian J. 1985 Observation of waves during oscillatory flow. *Journal of Fluid Mechanics* **151**, 395–426.

Stewartson, K & Stuart, J T 1971 A non-linear instability theory for a wave system in plane poiseuille. *Journal of Fluid Mechanics* **48**, 529–545.

Stuart, J T 1971 Nonlinear stability theory. *Annual Review of Fluid Mechanics* **3**, 347–370.

Tillmark, N. & Alfredsson, P. H. 1992 Experiments on transition in plane couette flow. *Journal of Fluid Mechanics* **235**, 89–102.

Trefethen, Lloyd N, Trefethen, Anne E, Reddy, Satish C & Driscoll, Tobin A 1993 Hydrodynamic stability without eigenvalues. *Science* **261**, 578–584.

Tutty, O. R. & Pedley, T. J. 1993 Oscillatory flow in a stepped channel. *Journal of Fluid Mechanics* **247**, 179–204.

Wright, T.G. & L.N.Trefethen 2002 Eigtool. *http://www.comlab.ox.ac.uk/psuedospectra/eigtool* .